phys. stat. sol. (a) **171**, 17 (1999)

Subject classification: 61.72.Lk; 61.72.Ji; 62.20.Fe; S5.11; S5.12; S6

Dislocation Kink Dynamics in Crystals with Deep Peierls Potential Relief

YU. L. IUNIN[1]) and V. I. NIKITENKO

Institute of Solid State Physics, Russian Academy of Sciences, 142 432 Chernogolovka, Moscow district, Russia

(Received September 7, 1998)

Processes of the nucleation and motion of kinks, determining the dislocation mobilities in crystals with high Peierls barriers, are reviewed. Various mechanisms of an influence of point defects on the kink dynamics are analyzed. To demonstrate these mechanisms experimental data are presented obtained with two-level intermittent loading of Si, Ge, and bulk SiGe alloy single crystals. The instability of a dislocation glide in SiGe crystals has been discovered, and modes are revealed of the linear and nonlinear kink drift. The experimental data are analyzed in the framework of models, considering the interaction of point defects with a dislocation and a kink.

1. Introduction

The dislocation motion in a deep potential relief of a perfect crystal lattice occurs by the formation and drift spreading of the kink pairs [1]. The theory of these processes has been well developed in different approximations [2 to 9]. However, a number of paradoxical discrepancies between the predictions of theory and experimental data have been discussed [10 to 12]. To solve the contradictions new approaches are necessary, taking into account the additional factors such as the influence of point defects on the kink pair formation and motion. Different models have been developed, considering, apart from the secondary Peierls relief, the point defect influence on the kink pair formation and motion (weak and strong obstacles, entrainment of point defects, field of random forces, etc.) [10, 11, 13 to 17].

To reveal which of the barriers is the dominant for a kink motion along a dislocation line in each case, one needs to study the kink dynamics experimentally. Recently the combination of high resolution electron microscopy and image processing allowed one to watch the motion of kinks along the dislocations in Si [18], Ge, and GaAs [19] single crystals. But this technique fails to provide a precise control of the uniformity of stress along the specimen.

The method of a two-level intermittent loading (TLIL) [20] allows one to study the processes of the kink pair formation and one-dimensional kink motion under well defined temperatures and low shear stresses when the kink motion is most sensitive to obstacles. This paper presents the results of a study of TLIL kink dynamics with Si, Ge and SiGe alloy specimens, revealing different modes of kink motion along the dislocation line. Besides their fundamental importance, such investigations are also significant for a study of mechanical properties of multilayered heterostructures [21].

[1]) e-mail: iunin@issp.ac.ru; Tel.: 7 (096) 524-9498; Fax: 7 (096) 576-4111.

2. Experimental

The investigated specimens were rectangular rods with edge orientations $[1\bar{1}0]$, $[11\bar{2}]$, and [111] and dimensions $35 \times 4 \times 1.5\ \text{mm}^3$. They were cut from Si, Ge, or SiGe alloy single crystal dislocation-free ingots. The silicon crystals were grown by the floating zone method. The germanium and $Si_{1-x}Ge_x$ ($0 < x < 0.15$) single crystals were grown by the Czochralski technique. The n-type silicon and germanium boules were doped with phosphorus (1.5 Ω m) and antimony (0.4 Ω m), respectively. The SiGe ingots were low doped with phosphorus or boron with a concentration of about $10^{15}\ \text{cm}^{-3}$.

The individual dislocation half-loops were produced by Vickers indentation on the (111) surface of a specimen at room temperature with subsequent deformation by four-point bending around the $[11\bar{2}]$ axis at 873 K (Si and SiGe) or 583 K (Ge). Dislocation displacements under subsequent loading were revealed by selective etching.

Significant starting stresses τ_s were revealed in SiGe specimens [22]. Theory [23] predicts that the value of τ_s depends on the state of the dislocation point defect atmosphere. To get the identical initial point defect atmosphere conditions for each loading, the preloading procedure has been used for all crystals, when the dislocations were displaced during 10 to 15 min under resolved shear stresses $\tau = 10$ MPa (Ge) and 30 MPa (Si and SiGe) and temperatures $T = 583$ K (Ge) and 873 K (Si and SiGe). To eliminate the possibility of dislocation immobilization in SiGe specimens a short pulse preloading has been also applied before each loading [22].

The TLIL method is based on the loading of a specimen containing individual dislocations by a sequence of stress pulses τ_i. We denote below the parameters for the pulse loading and pulse separation with the subscript indexes i and p, respectively, and the ones for the conventional steady state motion with st. The duration of an individual pulse t_i is comparable with $t_a = a/V_{st}$, being a mean time of the dislocation displacement for one lattice parameter a. The pulses are separated by "pauses" with duration t_p when either the stress is not applied at all ($\tau_p = 0$) or a small enough stress $\tau_p \ll \tau_i$ of the same or opposite sign with respect to τ_i is applied.

The specimens with individual dislocations were deformed by four-point bending around the $[11\bar{2}]$ axis by a sequence of pulses driven from a function generator with a required pulse ratio through an electromagnetic force transducer. The "pause" stress τ_p was produced by applying of a constant subloading using a six-point procedure being described in [24].

In order to determine the temporal characteristics of the kink pair formation and kink migration, the dependences of the average glide distances of 60° dislocations on the pulse separation $l(t_p)$ for a fixed duration of load pulses were measured. The total duration of the loading pulses Σt_i was equal to the static loading time t_{st}, at which dislocations moved over distances of 15 to 30 μm. The width of the leading edge of the load pulses was held constant ($t_f = 4$ ms). The temperature T was measured with a thermocouple placed next to the specimen and was kept constant and equal to (583 ± 1) K (Ge) or (873 ± 1) K (Si and SiGe).

3. Model of a Dislocation Motion under TLIL

During the pulse stress action, in addition to thermodynamically equlibrium kinks, extra kink pairs form and spread along the dislocation line. As the pulse separation goes on,

they become unstable and collapse to the formation centres under the action of the forces caused by the external stresses, mutual attraction of kinks, and the interaction of the dislocation and kink with point defects. The dislocation velocity V is proportional to the linear kink density c_k and the kink drift velocity V_k [1]:

$$V = ac_k V_k \,. \tag{1}$$

With low stresses being much less than the Peierls stress, the kink density c_k is close to the thermodynamically equilibrium value and is considered as being constant. When the directed drift motion of kinks prevails over the chaotic diffusion, one may estimate the average kink velocity during the cycle of TLIL with $(x_i + x_p)/(t_i + t_p)$ [25]. We suppose below $x_p < 0$. We receive with (1) the dislocation displacement under TLIL: $l = V\Sigma(t_i + t_p) = ac_k(x_i + x_p)/(t_i + t_p)\,\Sigma(t_i + t_p)$. Here $\Sigma(t_i + t_p) = N(t_i + t_p)$ is the loading duration. Assuming that the kink velocity under the pulse loading $x_i/t_i = V_k$, and $t_{st} = \Sigma t_i = Nt_i$, where N is the number of pulses, we receive

$$l/l_{st} = 1 + x_p/x_i \,. \tag{2}$$

The model thus relates immediately the microscopic kink displacements and experimentally observable macroscopic dislocation path lengths. This allows one to study experimentally different modes of the dislocation kink dynamics.

4. Kink Drift in a Random Potential

We now assume that a standard linear drift of kinks takes place during the pulse and pulse separation. This mode is realized either in the secondary Peierls relief of a perfect crystal [1], or in the random potential created by the interaction of a kink with point defects [10, 11]. The kink velocity is proportional to the applied shear stress and the kink mobility (D_k/kT)

$$V_k = (D_k/kT)\,\tau ab \,. \tag{3}$$

Here D_k is the kink diffusivity (being different in the perfect and random potential), b is the magnitude of the Burgers vector of a dislocation, and k is the Boltzmann constant. With $\tau_p < 0$ the equation (2) is reduced to the form

$$\frac{l}{l_{st}} = 1 - \frac{|v_p|\, t_p}{v_i t_i} \,. \tag{4}$$

Fig. 1 shows plots of the average dislocation glide distances in Si, normalized to the value with static loading, versus the relative pulse separation. The data with different "pause" shear stresses (τ_p) were obtained with a fixed pulse shear stress amplitude $(\tau_i = 7$ MPa) and fixed pulse durations. One can see that with the "pause" subloading with the stress of $\tau_p = -1.1$ MPa (curve 1) the glide distances may be approximated with a linear dependence. This result agrees qualitatively with (4). However, if we substitute values of τ_p and τ_i, used in experiment, into (4), the calculated decrease of dislocation displacements goes much slower than the experimental data. So we have to consider the existence of an additional driving force for the kink pair relaxation. This driving force has been attributed in [20] to the interaction between the dislocation and its Cottrell atmosphere. An inhomogeneous distribution of mobile point defects across the dislocation causes a local change in the dislocation energy and the appearance of

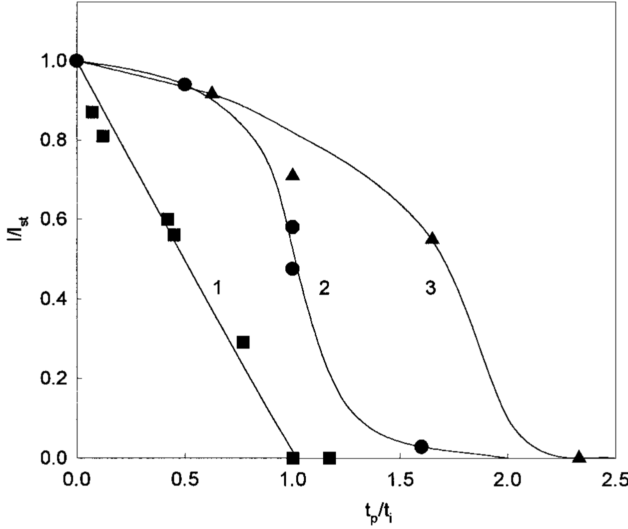

Fig. 1. Average normalized 60° dislocation glide distances in Si as a function of a relative pulse separation for different levels of stresses applied during the "pauses": (1) $\tau_p = -1.1$ MPa, $t_i = 30$ ms; (2) $\tau_p = 0$, $t_i = 30.9$ ms; (3) $\tau_p = +1$ MPa, $t_i = 130$ ms

additional internal stresses favoring the relaxation of the kink pair to its formation center (the dynamical starting stress) [26]:

$$\tau_s = (c_1 - c_2)\, u/(ab)\,. \tag{5}$$

Here c_1 and c_2 are the concentrations of point defects in adjacent valleys of the potential relief, u is the energy of a short-range interaction of a dislocation with a point defect. Within this assumption the kink drift velocity during the pulse is $v_i \sim (\tau_i - \tau_s)$ and the one during the pause is $v_p \sim (\tau_p + \tau_s)$, and the experimental data (Fig. 1, curve 1) may be described with (4) and $\tau_s = 2.9$ MPa. However, with larger $\tau_p \geq 0$ (Fig. 1, curves 2, 3) the dependences $l(t_p)$ are S-shaped and have points of inflection. A threshold-type drop of displacements down to zero is observed at larger t_p.

5. Effects of Entrainment of Point Defects by a Dislocation

5.1 Immobilization of a dislocation

This effect may be explained [27] as a result of the interaction of a moving dislocation with a point defect atmosphere. The redistribution of mobile point defects, surrounding a dislocation, leads to the starting stress dependence on the dislocation velocity. The value of $\Delta c = (c_1 - c_2)$ depends on the point defect mobility and the dislocation velocity value [23] as

$$\Delta c = c_0[\exp\,(a/Vt_m) - 1] \approx c_0 a/Vt_m\,. \tag{6}$$

Here t_m is the characteristic time of the point defect displacement for one lattice parameter; c_0 is the average concentration of point defects in a crystal. It was supposed also that $t_m > t_a$. One can see that the less is V, the greater is Δc and, hence (5), the τ_s.

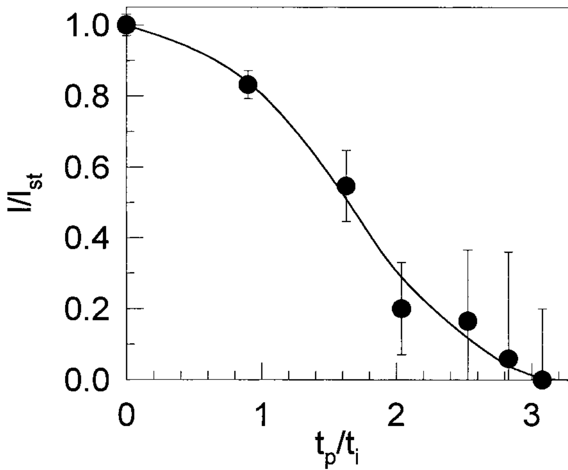

Fig. 2. Normalised 60° dislocation displacement vs. relative pulse separation in bulk SiGe single crystals with Ge content of 2 at%, $t_i = 20$ ms, $t_i/t_a = 0.8$, $\tau_i = 15$ MPa, $\tau_p = 0$

Let us suggest that the dislocation velocity is proportional to the average shear stress $\langle\tau\rangle$ acting upon a dislocation during the TLIL period. The values of $\langle\tau\rangle$ and V decrease, so τ_s increases with (t_p/t_i) increase. We may conclude that there exists a critical value of t_p^* when the avalanche accumulation of point defects should occur. With $t_p > t_p^*$ the steady state dislocation motion is impossible and the immobilization of dislocations occurs. This allows one to explain qualitatively a sharp decrease of the dislocation mobility with larger pulse separations.

A similar effect of dislocation immobilization has been observed also in TLIL experiments with SiGe specimens having a Ge content of 2 at% (Fig. 2). We found, however, that the variation of the Ge content changes the dislocation and kink mobility modes in SiGe drastically.

5.2 *Instability of dislocation glide*

Apart from the steady state dislocation motion and the dislocation immobilization due to the avalanche accumulation of point defects, one more mode of dislocation motion in SiGe alloy has been revealed. Fig. 3 presents a picture of the (111) surface of a SiGe specimen. After the dislocations were produced, the specimen has been loaded during 30 min with τ = 30 MPa at 873 K. A surface layer of about 10 μm has been removed by chemical polishing and the specimen was chemically etched after a cooling during 1 h. One can see two large etch pits revealing the positions of screw dislocations and many flat bottom etch pit traces behind them. The surface-by-surface removal of layers by chemical polishing with subsequent selective etching shows that the traces go parallel to the dislocation lines, i.e., coincide with the location of dislocation lines during their glide.

Similar etch pits were observed earlier in Si and Ge specimens when the dislocations increased their velocities with the abrupt variation of the applied shear stress [24, 28]. The flat-bottom etch pits were concluded to be the linear defects formed by a part of the dislocation point defect atmosphere being lost with the dislocation acceleration. In our case, however, these traces are formed under steady loading. So we have to conclude that dislocations loose part of their point defect atmosphere and, according to

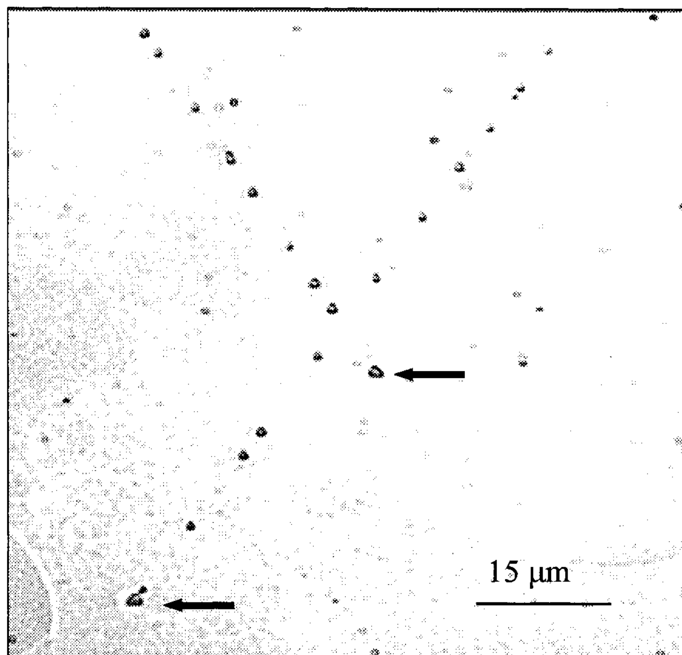

Fig. 3. The (111) surface of a SiGe specimen (1 at% Ge) after removal of a layer of 10 μm and selective chemical etching. The arrows show two large etch pits revealing the screw dislocations, many flat bottom etch pits beyond them reveal the traces

(6), change their velocity regularly. We may conclude that relaxational oscillations of the dislocation velocity occur.

A possible reason of the variation of the dislocation velocity may be the accumulation of mobile defects with the dislocation motion in a specimen being saturated with point defects. Point defects are the obstacles for the kink motion [13]. The higher is the accumulated point defect density, the slower is the kink motion. So the probability increases of a second kink pair formation before the annihilation of kinks of a first pair occurs, and the superkinks of a double height form. This allows dislocations to move for two lattice parameters at once and to detach from point defects, having no time to jump for two lattice parameters. These accumulated and lost point defects form the linear region being revealed with the chemical etching. This version is confirmed also by the fact that the traces could not be more revealed after the treatment of a specimen at 700 to 900 K for about 6 h. Probably the concentration of point defects decreases due to the formation of complexes of point defects and diffusion to the specimen surface, dislocations, and other structure defects.

6. Kink Drift in the Field of Random Forces

Unlike silicon, there are no starting stresses for the dislocation motion in low doped germanium crystals. So the entrainment of point defects is insignificant and one may study the modes of kink migration under low shear stresses, when the influence of

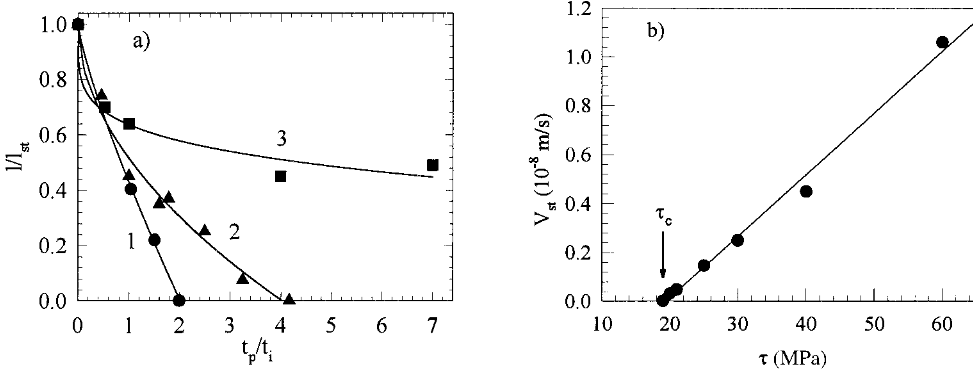

Fig. 4. a) Normalised 60° dislocation displacement in Ge vs. relative pulse separation: (1) $\tau_p = -8$ MPa, $t_i = 45$ ms; (2) $\tau_p = -4$ MPa, $t_i = 48$ ms; (3) $\tau_p = 0$, $t_i = 30$ ms, $\tau_i = 30$ MPa. b) Stress dependence of the average 60° dislocation velocity in Ge

point defects on the kink drift is most pronounced. Fig. 4a shows how the dependences of mean dislocation glide distances in Ge on the relative pulse separation change with the shear stress in the pause increase. One can see that the decrease of dislocation glide distances is nonlinear, especially for small τ_p values, as opposed to the predictions of a model of the linear kink drift (4). So we have to conclude that a concept of "weak obstacles" (dragging points), forming the random potential for the kink motion [10, 11, 13] and determining the linear kink drift, is not applicable for our experimental data.

Another approach concentrates on a short-range interaction of point defects with the dislocation line [13, 14, 17], but not with the kink itself. The attachment of point defects to the dislocation core or their detachment with a kink motion causes an abrupt change in the energy of a dislocation and hence the specific step-like dependence of the energy of a kink pair on its size (Fig. 5). Because of the co-operative effect of numerous point defects this interaction is more pronounced with small defect concentration than the one considering the kink interaction with separate defects [10, 11, 13]. The interaction of a dislocation with manifold point defects leads to the existence of a critical shear stress τ_c separating two different modes of the dislocation kink motion. With $\tau > \tau_c$ the

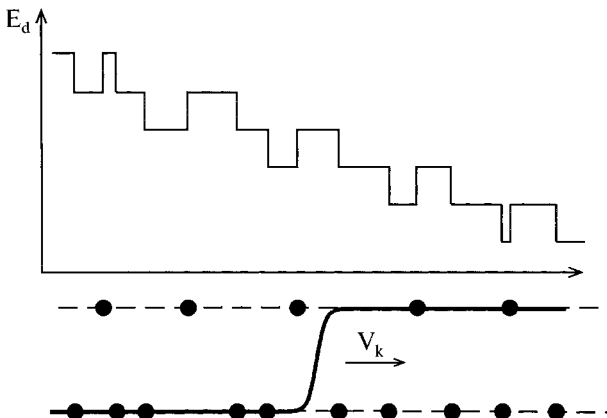

Fig. 5. Kink motion in a field of random forces

linear drift $x = V_k t$ takes place, with

$$V_k = (D_k/kT)\,(\tau - \tau_c)\,ab\,. \tag{7}$$

This expression points to an existence of the dislocation kink mobility threshold with $\tau = \tau_c$. Actually kinks do not stop with $\tau < \tau_c$, but the sublinear dependence of the kink path length x on time t takes place with the drift in the field of random forces

$$x = x_0(t/t_0)^\delta\,, \qquad \delta = \tau/\tau_0 \le 1\,, \tag{8}$$

$$x_0 = kT/\tau_0 ab\,, \quad \tau_0 = (c_1 + c_2)\,u^2/(2kTa^2b)\,, \quad t_0 = x_0^2/2D_k\,, \quad \tau_c \approx \tau_0 + \tau_s\,. \tag{9}$$

We found that our data on the stress dependence of the dislocation velocity in Ge under conventional loading may be described satisfactorily with (1), with V_k being determined by (7) and $\tau_c = 19$ MPa (solid line in Fig. 4b). In our experiments $\tau_i > \tau_c$, and a linear drift (7) takes place during a pulse. All values of $\tau_p < \tau_c$, so we use (8) for the kink displacements during the pause. We receive then with (2)

$$l/l_{st} = 1 - K(t_p/t_i)^\delta\,, \tag{10}$$

$$\delta = \frac{\tau_p + \tau_s}{\tau_0}\,, \qquad K = \frac{\tau_0}{\tau_i - \tau_c}\left(\frac{t_0}{t_i}\right)^{1-\delta}\,. \tag{11}$$

Let us compare the experimental data of Fig. 4a with the model (10), (11). The solid lines in Fig. 4a are plotted with (10), with δ and t_0 being fitting parameters. One can see satisfactory agreement of the theory with experiment.

To check the validity of the model, the results of fitting several TLIL experiments were replotted within the coordinates δ versus $(\tau_p + \tau_s)$ (Fig. 6). According to (11), the dependence should be linear with a slope of $1/\tau_0$. One can see good agreement between theory and experimental data. The second fitting parameter t_0 allows one to estimate the kink diffusivity with (9) and the kink migration enthalpy with the expression [1] $W_m = kT \ln(\nu_D b^2/D_k)$, where ν_D is the Debye frequency. All the calculated values are in the range $W_m = (1 \pm 0.1)$ eV, those are in reasonable agreement with the ones obtained by other authors [29, 30].

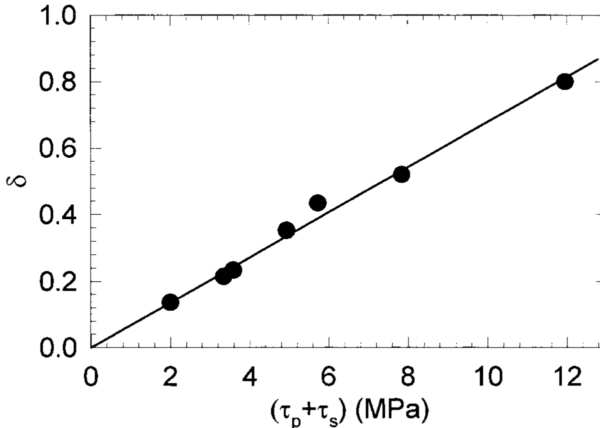

Fig. 6. Stress dependence of parameter δ

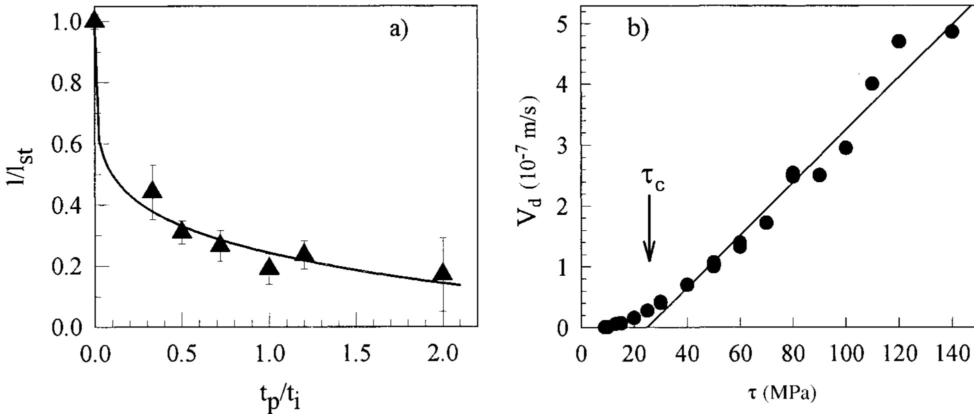

Fig. 7. a) Normalised 60° dislocation displacement vs. relative pulse separation in bulk SiGe single crystals with a Ge content of 5.5 at%, $t_i = 30$ ms, $t_i/t_a = 0.83$, $\tau_i = 15$ MPa. b) Stress dependence of the individual dislocation velocity in SiGe

Similar results were obtained with SiGe specimens containing 5.5 at% Ge (Fig. 7a). To check the possibility of a description of these data with the model of kink motion in the field of random forces, we plotted the stress dependence of the individual dislocation velocity (Fig. 7b). One can see that at stresses above 40 MPa the dislocation velocity is well described with (1) with V_k being determined by (7) and $\tau_c = 25$ MPa. Both τ_i and τ_p are less than τ_c, so the kink drift is nonlinear during all the pulse loading cycle. Using (8) both for x_i and x_p and substituting them into (2), we receive

$$l/l_{st} = 1 - K(t_p/t_i)^{\delta_p} \tag{12}$$

with $\delta_p = \tau_s/\tau_0$, $K = (t_0/t_i)^{\delta_i - \delta_p}$, $\delta_i = (\tau_i - \tau_s)/\tau_0$. The solid line in Fig. 7a shows the result of fitting the experimental data with (12). One can see that theory and experiment agree well. The fitting parameter t_0 allows one to estimate the kink diffusivity with (9) and the kink migration enthalpy $W_m \approx 1.6$ eV. The estimated value is in reasonable agreement with the ones obtained for the dislocation kinks in pure Si [31, 32].

7. Conclusion

It is shown that the point defect atmosphere not only determines the barriers for the kink motion, but also stimulates the kink pair return to the formation centers. The entrainment of point defects may cause both the dislocation immobilization and the instability of dislocation glide. With high shear stresses the conventional linear kink drift takes place. With low stresses the specific mode of a kink drift along the dislocation line is observed.

Acknowledgements The authors are grateful to Dr. B. Ya. Farber, Prof. A. Heuer, Dr. B. V. Petukhov, Prof. P. Pirouz, and Dr. V. I. Orlov for useful discussions, to Dr. N. V. Abrosimov for supplying with SiGe crystals, and to D. V. Dyachenko-Dekov for help with obtaining some results with SiGe crystals. This work was partly supported by INTAS grant No. 96-363.

References

[1] J. P. Hirth and J. Lothe, Theory of Dislocations, McGraw-Hill Publ. Co., New York 1982.
[2] J. Lothe and J. P. Hirth, Phys. Rev. **115**, 543 (1959).
[3] A. Seeger and P. Schiller, in: Physical Acoustics, Vol. IIIA, Ed. W. P. Mason, Academic Press, New York/London 1966 (p. 351).
[4] A. P. Kazantzev and V. L. Pokrovskii, Soviet Phys. – J. Exper. Theor. Phys. **31**, 362 (1970).
[5] B. V. Petukhov and V. L. Pokrovskii, Soviet Phys. – J. Exper. Theor. Phys. **36**, 336 (1973).
[6] M. Büttiker and R. Landauer, Phys. Rev. **23**, 1397 (1981).
[7] V. V. Bulatov, S. Yip, and A. S. Argon, Phil. Mag. A **72**, 453 (1995).
[8] Y. M. Huang, J. C. H. Spence, and O. F. Sankey, Phys. Rev. Lett. **74**, 3392 (1995).
[9] R. W. Nunes, J. Bennetto, and D. Vanderbilt, Phys. Rev. B **57**, 10388 (1998).
[10] V. Celli, M. N. Kabler, T. Ninomiya, and R. Thomson, Phys. Rev. **131**, 58 (1963).
[11] V. V. Rybin and A. N. Orlov, Soviet Phys. – Solid State **11**, 2635 (1969).
[12] V. I. Nikitenko and B. Ya. Farber, in: Proc. 9th Yamada Conf. Dislocations in Solids, Tokyo, 1985 (p. 417).
[13] B. V. Petukhov, Soviet Phys. – Solid State **13**, 1204 (1971).
[14] H. Suzuki, in: Dislocations in Solids, Vol. 4, Dislocations in Metallurgy, North-Holland Publ. Co., Amsterdam 1979 (p. 191).
[15] M. Heggie and R. Jones, Phil. Mag. B **48**, 365 (1983).
[16] V. M. Vinokur, J. Physique **47**, 1425 (1986).
[17] J. P. Bouchaud and A. Georges, Comments Condens. Matter Phys. **15**, 125 (1991).
[18] H. R. Kolar, J. C. H. Spence, and H. Alexander, Phys. Rev. Lett. **77**, 4031 (1996).
[19] K. Maeda, M. Inoue, K. Suzuki, H. Amasuga, M. Nakamura, and E. Kanematsu, J. Physique III **7**, 1451 (1997).
[20] Yu. L. Iunin, V. I. Nikitenko, V. I. Orlov, and B. Ya. Farber, Soviet Phys. – J. Exper. Theor. Phys. **73**, 1079 (1991).
[21] R. Hull and J. C. Bean, phys. stat. sol. (a) **138**, 533 (1993).
[22] Yu. L. Iunin, V. I. Orlov, D. V. Dyachenko-Dekov, N. V. Abrosimov, S. N. Rossolenko, and W. Schröder, Solid State Phenomena **57,** 419 (1997).
[23] B. V. Petukhov, Soviet Phys. – Tekh. Phys. **35**, 1150 (1990).
[24] V. I. Nikitenko, B. Ya. Farber, and I. E. Bondarenko, Soviet Phys. – J. Exper. Theor. Phys. **55**, 891 (1982).
[25] B. V. Petukhov and Yu. A. Polyakov, Soviet Phys. – Crystallography **37**, 144 (1992).
[26] B. V. Petukhov, Soviet Phys. – Solid State **30**, 1669 (1988).
[27] Yu. L. Iunin, V. I. Nikitenko, V. I. Orlov, and B. V. Petukhov, in: Strength of Materials, Proc. ICSMA-10, Ed. H. Oikawa, K. Maruyama, S. Takeuchi, and M. Yamaguchi, Sendai 1994 (p. 101).
[28] V. I. Nikitenko, B. Ya. Farber, and E. B. Yakimov, J. Physique **44**, C4–85 (1983).
[29] F. Louchet, D. Cochet Muchy, Y. Brechet, and J. Pelissier, Phil. Mag. A **57**, 327 (1988).
[30] U. Jendrich and P. Haasen, phys. stat. sol. (a) **108**, 553 (1988).
[31] F. Louchet, Phil. Mag. A **43**, 1289 (1981).
[32] B. Ya. Farber, Yu. L. Iunin, and V. I. Nikitenko, phys. stat. sol. (a) **97**, 469 (1986).